# Tau Decays with One Charged Particle Plus Multiple $\pi^0$'s

M. Procario,[1] S. Yang,[1] R. Balest,[2] K. Cho,[2] M. Daoudi,[2] W. T. Ford,[2] D. R. Johnson,[2] K. Lingel,[2] M. Lohner,[2] P. Rankin,[2] J. G. Smith,[2] J. P. Alexander,[3] C. Bebek,[3] K. Berkelman,[3] D. Besson,[3] T. E. Browder,[3] D. G. Cassel,[3] H. A. Cho,[3] D. M. Coffman,[3] P. S. Drell,[3] R. Ehrlich,[3] R. S. Galik,[3] M. Garcia-Sciveres,[3] B. Geiser,[3] B. Gittelman,[3] S. W. Gray,[3] D. L. Hartill,[3] B. K. Heltsley,[3] K. Honscheid,[3] C. D. Jones,[3] S. L. Jones,[3] J. Kandaswamy,[3] N. Katayama,[3] P. C. Kim,[3] D. L. Kreinick,[3] G. S. Ludwig,[3] J. Masui,[3] J. Mevissen,[3] N. B. Mistry,[3] C. R. Ng,[3] E. Nordberg,[3] M. Ogg,[3,a] C. O'Grady,[3] J. R. Patterson,[3] D. Peterson,[3] D. Riley,[3] M. Sapper,[3] M. Selen,[3] H. Worden,[3] M. Worris,[3] F. Würthwein,[3] P. Avery,[4] A. Freyberger,[4] J. Rodriguez,[4] R. Stephens,[4] J. Yelton,[4] D. Cinabro,[5] S. Henderson,[5] K. Kinoshita,[5] T. Liu,[5] M. Saulnier,[5] R. Wilson,[5] H. Yamamoto,[5] A. J. Sadoff,[6] R. Ammar,[7] S. Ball,[7] P. Baringer,[7] D. Coppage,[7] N. Copty,[7] R. Davis,[7] N. Hancock,[7] M. Kelly,[7] N. Kwak,[7] H. Lam,[7] Y. Kubota,[8] M. Lattery,[8] J. K. Nelson,[8] S. Patton,[8] D. Perticone,[8] R. Poling,[8] V. Savinov,[8] S. Schrenk,[8] R. Wang,[8] M. S. Alam,[9] I. J. Kim,[9] B. Nemati,[9] J. J. O'Neill,[9] V. Romero,[9] H. Severini,[9] C. R. Sun,[9] M. M. Zoeller,[9] G. Crawford,[10] R. Fulton,[10] K. K. Gan,[10] H. Kagan,[10] R. Kass,[10] J. Lee,[10] R. Malchow,[10] F. Morrow,[10] Y. Skovpen,[10,b] M. Sung,[10] C. White,[10] J. Whitmore,[10] P. Wilson,[10] F. Butler,[11] X. Fu,[11] G. Kalbfleisch,[11] M. Lambrecht,[11] W. R. Ross,[11] P. Skubic,[11] J. Snow,[11] P. L. Wang,[11] M. Wood,[11] D. Bortoletto,[12] D. N. Brown,[12] J. Dominick,[12] R. L. McIlwain,[12] T. Miao,[12] D. H. Miller,[12] M. Modesitt,[12] S. F. Schaffner,[12] E. I. Shibata,[12] I. P. J. Shipsey,[12] P. N. Wang,[12] M. Battle,[13] J. Ernst,[13] H. Kroha,[13] S. Roberts,[13] K. Sparks,[13] E. H. Thorndike,[13] C. H. Wang,[13] S. Sanghera,[14] T. Skwarnicki,[14] R. Stroynowski,[14] M. Artuso,[15] D. He,[15] M. Goldberg,[15] N. Horwitz,[15] R. Kennett,[15] G. C. Moneti,[15] F. Muheim,[15] Y. Mukhin,[15] S. Playfer,[15] Y. Rozen,[15] P. Rubin,[15] S. Stone,[15] M. Thulasidas,[15] G. Vasseur,[15] W. M. Yao,[15] G. Zhu,[15] A. V. Barnes,[16] J. Bartelt,[16] S. E. Csorna,[16] Z. Egyed,[16] V. Jain,[16] P. Sheldon,[16] D. S. Akerib,[17] B. Barish,[17] M. Chadha,[17] S. Chan,[17] D. F. Cowen,[17] G. Eigen,[17] J. S. Miller,[17] J. Urheim,[17] A. J. Weinstein,[17] D. Acosta,[18] M. Athanas,[18] G. Masek,[18] B. Ong,[18] H. Paar,[18] M. Sivertz,[18] A. Bean,[19] J. Gronberg,[19] R. Kutschke,[19] S. Menary,[19] R. J. Morrison,[19] H. N. Nelson,[19] J. D. Richman,[19] H. Tajima,[19] D. Schmidt,[19] D. Sperka,[19] and M. S. Witherell[19]

(CLEO Collaboration)

[1]*Carnegie-Mellon University, Pittsburgh, Pennsylvania 15213*
[2]*University of Colorado, Boulder, Colorado 80309-0390*
[3]*Cornell University, Ithaca, New York 14853*
[4]*University of Florida, Gainesville, Florida 32611*
[5]*Harvard University, Cambridge, Massachusetts 02138*
[6]*Ithaca College, Ithaca, New York 14850*
[7]*University of Kansas, Lawrence, Kansas 66045*
[8]*University of Minnesota, Minneapolis, Minnesota 55455*
[9]*State University of New York at Albany, Albany, New York 12222*
[10]*Ohio State University, Columbus, Ohio, 43210*
[11]*University of Oklahoma, Norman, Oklahoma 73019*
[12]*Purdue University, West Lafayette, Indiana 47907*
[13]*University of Rochester, Rochester, New York 14627*
[14]*Southern Methodist University, Dallas, Texas 75275*
[15]*Syracuse University, Syracuse, New York 13244*
[16]*Vanderbilt University, Nashville, Tennessee 37235*
[17]*California Institute of Technology, Pasadena, California 91125*
[18]*University of California, La Jolla, California 92093*
[19]*University of California at Santa Barbara, Santa Barbara, California 93106*

(Received 2 October 1992)

With the CLEO-II detector at the Cornell Electron Storage Ring, we have measured branching fractions for tau lepton decay into one-prong final states with multiple $\pi^0$'s, $B_{hn\pi^0}$, normalized to the branching fraction for tau decay into one charged particle and a single $\pi^0$. We find $B_{h2\pi^0}/B_{h\pi^0}=0.345\pm0.006\pm0.016$, $B_{h3\pi^0}/B_{h\pi^0}=0.041\pm0.003\pm0.005$, and $B_{h4\pi^0}/B_{h\pi^0}=0.006\pm0.002\pm0.002$.

PACS numbers: 13.35.+s, 14.60.Jj

The existing data for branching ratios of tau decays to final states containing multiple $\pi^0$'s are relatively imprecise [1]. Improved measurements are essential to help resolve the long-standing "one-prong problem" in tau decays [2,3], wherein exclusive modes fail to saturate the inclusive one-charged-particle decay width. In this Letter, we present precise measurements of the branching fractions $B_{hn\pi^0} \equiv B(\tau^{\pm} \to h^{\pm} n\pi^0 \nu_\tau)$ for $n=2$ and 3, and the first measurement of $B(\tau^{\pm} \to h^{\pm} 4\pi^0 \nu_\tau)$, where $h^{\pm}$ represents a charged hadron ($\pi^{\pm}$ or $K^{\pm}$). We normalize these branching fractions to $B(\tau^{\pm} \to h^{\pm}\pi^0\nu_\tau)$, since many systematic errors are common to both measurements and will largely cancel in their ratio.

The data were recorded using the CLEO-II detector at the Cornell Electron Storage Ring (CESR). CLEO-II is a solenoidal-magnet spectrometer and electromagnetic calorimeter [4]. Reconstruction of multiple $\pi^0 \to \gamma\gamma$ decays is made possible by the high efficiency, excellent energy resolution, and fine segmentation of the calorimeter, which consists of 7800 CsI(Tl) crystals located inside the magnet. The data sample is obtained from $e^+e^-$ collisions at a center-of-mass energy $E_{\rm c.m.} \sim 10.6$ GeV, with an integrated luminosity of 670 pb$^{-1}$, corresponding to $\sim 610\,000$ produced $\tau^+\tau^-$ pairs.

To study multi-$\pi^0$ $\tau$ decays, we identify the decay of the recoiling ("tag") $\tau$. In this Letter, we describe two independent analyses: one using leptonic ($e\nu\bar{\nu}$, $\mu\nu\bar{\nu}$) tags; and one using three-prong ($3h^{\pm}[\pi^0]\nu$) tags. We select events with 1-1 and 1-3 charged-track topologies and zero net charge. The opening angle between the charged tracks in the 1-1 topology must exceed 90°; 1-3 events are divided into two hemispheres by the plane perpendicular to the highest momentum track. Only one track may have more than 85% of the beam momentum, and at least two tracks must project back to the $e^+e^-$ interaction point. For leptonic (three-prong) tags, the total energy deposited in the calorimeter must be less than $0.85E_{\rm c.m.}$ ($0.75E_{\rm c.m.}$), and the total visible energy $E_{\rm vis}$ must exceed $0.2E_{\rm c.m.}$ ($0.3E_{\rm c.m.}$), assuming all observed charged particles to be pions.

We identify electrons above 0.5 GeV/$c$ using energy measurements from the calorimeter and momentum and specific ionization measurements from the tracking system. Muons above 1.0 GeV/$c$ are identified by projecting tracks to hits in proportional tubes behind at least three absorption lengths of iron. We reject QED backgrounds to lepton tags by requiring the missing momentum to point into the detector, the net transverse momentum of the tracks to be above 200 MeV/$c$, and the ratio of the vector to scalar sum of the charged-track momenta to exceed 0.05.

For three-prong-tagged events, we reduce hadronic ($e^+e^- \to q\bar{q}$) background by requiring that the three-prong hemisphere contain no more than two photons (as defined below), that the missing mass, $[(E_{\rm c.m.} - E_{\rm vis})^2 - \mathbf{p}_{\rm vis}^2]^{1/2}$, be between 0.5 and 7.0 GeV/$c^2$, and that the invariant mass of all detected particles in each hemisphere be less than 1.7 GeV/$c^2$. The net momentum in each hemisphere must also point into the barrel region (defined below). We reject radiative Bhabha events with converted photons by allowing no more than one identified electron.

Photons are formed from clusters of crystal hits in the barrel ($|\cos\theta| < 0.80$) and end cap ($0.80 < |\cos\theta| < 0.95$) regions of the calorimeter, where $\theta$ is the angle with respect to the beam axis. We ignore clusters due to charged-particle interactions. For lepton tags, we also ignore those lying within 20° of the lepton's initial direction. We form $\pi^0$'s using only barrel photons with energy $E_\gamma > 60$ MeV. For lepton-tagged $\tau \to h^{\pm}4\pi^0\nu_\tau$ decays, we also use those with $30 < E_\gamma < 60$ MeV to improve the acceptance. In the three-prong analysis, we use photons in the signal (one-prong) hemisphere only; for lepton tags, the angle between paired photons may be as large as 135°, but the $\pi^0$ momentum must lie in the charged hadron hemisphere, and at least one photon must have $E_\gamma > 80$ MeV. These requirements minimize confusion from photons associated with the tag tau, and from low-energy clusters arising from beam-related processes unrelated to the tau pair.

To suppress contamination from other tau decays, the energy of any unused barrel photon may not exceed 100 (60) MeV in the lepton- (three-prong-) tagged analysis. Since we do not form $\pi^0$'s from endcap photons (because of poorer resolution and larger backgrounds), we veto events with appreciable energy deposition there.

In Fig. 1 we demonstrate the reconstruction of multiple $\pi^0$'s by plotting the invariant mass of one pair of photons versus that of a second pair. In the 3- and 4-$\pi^0$ cases, the remaining photon pair(s) must reconstruct to the $\pi^0$ mass, and plots from corresponding sideband regions have been subtracted to account for incorrect pairings of the remaining photons.

To extract the numbers of signal events, for each $\pi^0$ multiplicity hypothesis we select that combination of $\pi^0$ candidates with the smallest $n\pi^0$ chi-square, $\chi^2_{n\pi^0} = \sum_{i=1}^{n} (m_i - m_{\pi^0})^2/\sigma^2_{m_i}$. Here $m_i$ is the effective mass of the two photons forming the $i$th $\pi^0$ candidate, and $\sigma_{m_i}$ is the uncertainty on $m_i$ (typically 6–8 MeV/$c^2$) based on measured angular and energy resolutions of the calorimeter. In Fig. 2(a) we plot $m_{\gamma\gamma}$ for lepton-tagged events with two photons after this selection; we define the signal region to be $|m_{\gamma\gamma} - m_{\pi^0}| < 4\sigma_m$. In Figs. 2(b)–2(d) we plot the reduced $\chi^2_{n\pi^0}$ for the 2-, 3-, and 4-$\pi^0$ lepton-tagged data (points) and Monte Carlo (solid) samples, with arrows indicating locations of cuts [5]. The numbers of events in each sample are given in Table I. The $\pi^{\pm}(n\pi^0)$ invariant mass spectra for events from all tags are shown in Fig. 3.

The final samples contain background from several sources. We evaluate the contamination from events in which unrelated photons form a $\pi^0$ ($f_{\pi^0}$), from the tails of the $\chi^2$ distributions [6]. After accounting for $f_{\pi^0}$, residual hadronic background ($f_h$) in the lepton-tagged sample is

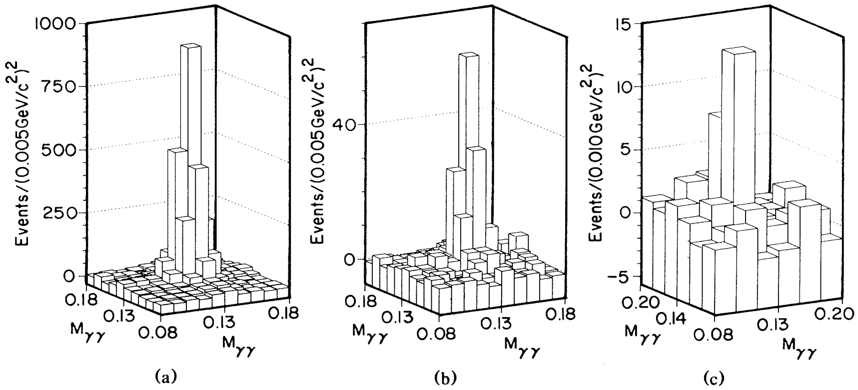


FIG. 1. Invariant mass of one pair of photons (randomly selected) vs that of a second pair for events in the lepton-tagged (a) 2-, (b) 3-, and (c) 4-$\pi^0$ samples, with one entry for each distinct combination of $n$ photon pairs in an event. In (b) and (c), the remaining photon pair(s) must have $|m_{\gamma\gamma}-m_{\pi^0}|<4\sigma_m$ (see text), and appropriately scaled plots have been subtracted in which the remaining pair(s) fail to reconstruct to the $\pi^0$ mass.

estimated from a Monte Carlo simulation. We determine $f_h$ for three-prong tags from the data, by selecting hadronic events using the 1-3 $\tau$ selection criteria described earlier, but requiring the mass of the $3h^{\pm}$ candidate to exceed 2.0 GeV/$c^2$, and permitting any number of photons in the three-prong hemisphere. We find $13\,322 \pm 115$ such events, of which $(9.8\pm0.3)\%$ are estimated from Monte Carlo simulation to be mismeasured $\tau$-pair events. As the invariant masses of the two hemispheres are not strongly correlated, we obtain the hadronic background in the three-prong-tagged $\tau$ sample by normalizing the one-prong mass ($M_1$) spectrum of the hadronic events to that of the $\tau$ candidates in a region ($M_1>2.0$ GeV/$c^2$) dominated by hadrons. The resulting values of $f_h$ are given for each $\pi^0$ multiplicity in Table I.

We determine detection efficiencies and background from other $\tau$ decays ($f_\tau$) based on Monte Carlo–simulated $\tau$-pair events. The kinematics of $\tau$-pair production and decay are generated with the KORALB [7] Monte Carlo program. These events are processed through a detector simulation based on the GEANT [8] program. Efficiencies relative to $h^{\pm}\pi^0\nu$ decays [9] are also given in Table I, along with values of $f_\tau$. Some contributions to $f_\tau$ are illustrated in Table II [10], where probabilities of reconstructing several $\tau$ decays as $h^{\pm}n\pi^0\nu$ are given for $\mu$-tagged events.

Branching fractions for the multi-$\pi^0$ $\tau$ decays are computed using the numbers of selected events, efficiencies

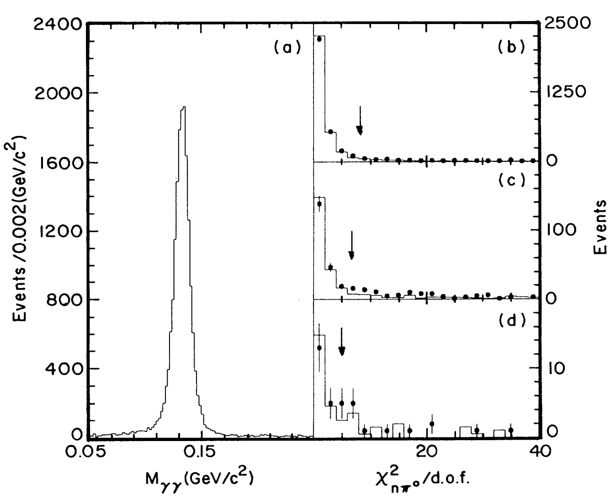


FIG. 2. Reconstruction of $\pi^0\to\gamma\gamma$ decays in lepton-tagged event samples: (a) the invariant mass of the two photons in the 1-$\pi^0$ data sample; (b)–(d) the $\chi^2_{n\pi^0}$ per degree of freedom (see text) for $n=2,3,4$ for events (points) with arrows indicating cuts. Monte Carlo distributions (solid histogram) are overlaid.

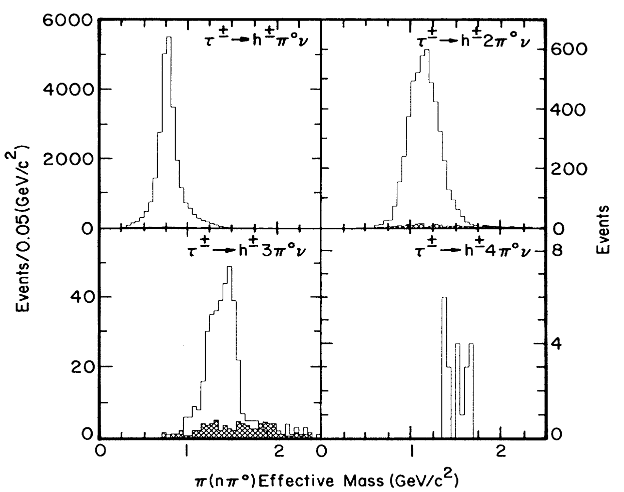


FIG. 3. Invariant $\pi^{\pm}n\pi^0$ mass spectra. Data from leptonic and three-prong tags are combined for events in the 1-, 2-, and 3-$\pi^0$ samples. The hatched histograms represent the spectra expected from hadronic background entering the three-prong sample. Only lepton-tagged events are shown for the $4\pi^0$ case.

TABLE I. Numbers of events, background fractions, relative detection efficiencies, and branching ratios for the $n$-$\pi^0$ candidate samples in the electron, muon, and three-prong-tagged analyses. Errors are statistical only.

| Mode ($X$) | Tag | Events | Backgrounds (%) $f_{\pi^0}$ | $f_h$ | $f_\tau$ | Relative efficiency (%) | $\frac{B(\tau \to X)}{B(\tau \to h^\pm \pi^0 \nu)}$ |
|---|---|---|---|---|---|---|---|
| | $e$ | 8935 | $2.2 \pm 0.1$ | $<0.1$ | $4.3 \pm 0.1$ | 100 | 1 |
| $h^\pm \pi^0 \nu$ | $\mu$ | 7470 | $2.3 \pm 0.1$ | $<0.1$ | $4.6 \pm 0.2$ | 100 | 1 |
| | $3h$ | 8511 | $2.0 \pm 0.1$ | $2.6 \pm 0.1$ | $3.4 \pm 0.2$ | 100 | 1 |
| | $e$ | 1639 | $4.1 \pm 0.3$ | $<0.4$ | $3.6 \pm 0.2$ | $53.8 \pm 0.8$ | $0.336 \pm 0.011$ |
| $h^\pm 2\pi^0 \nu$ | $\mu$ | 1434 | $3.7 \pm 0.3$ | $<1.0$ | $4.4 \pm 0.3$ | $53.3 \pm 0.8$ | $0.356 \pm 0.012$ |
| | $3h$ | 1561 | $2.9 \pm 0.2$ | $5.1 \pm 0.4$ | $3.0 \pm 0.2$ | $51.2 \pm 0.7$ | $0.347 \pm 0.011$ |
| | $e$ | 111 | $11 \pm 2$ | $<6$ | $12.4 \pm 1.7$ | $25.4 \pm 0.9$ | $0.041 \pm 0.004$ |
| $h^\pm 3\pi^0 \nu$ | $\mu$ | 100 | $11 \pm 2$ | $<6$ | $11.4 \pm 1.7$ | $27.0 \pm 1.0$ | $0.042 \pm 0.005$ |
| | $3h$ | 95 | $14 \pm 2$ | $22 \pm 3$ | $6.6 \pm 1.2$ | $19.5 \pm 0.8$ | $0.039 \pm 0.007$ |
| | $e$ | 9 | $14 \pm 6$ | $<10$ | $5.7 \pm 3.2$ | $16.8 \pm 1.1$ | $0.005 \pm 0.002$ |
| $h^\pm 4\pi^0 \nu$ | $\mu$ | 12 | $15 \pm 6$ | $<10$ | $4.3 \pm 2.3$ | $18.9 \pm 1.3$ | $0.007 \pm 0.003$ |
| | $3h$ | 4 | $45 \pm 27$ | $<45$ | $6 \pm 6$ | $6.3 \pm 0.9$ | $<0.012$(90% C.L.) |

and background contributions listed in Table I. Since the ratios of the multi-$\pi^0$ branching fractions enter explicitly in the estimate of $f_\tau$, we iterate until consistency is reached [11]. The final column of Table I lists the resulting ratios of branching fractions.

The dominant source of systematic uncertainty in both leptonic- and three-prong-tagged analyses is the $n\pi^0$-finding efficiency. The uncertainty in this efficiency arises from possible deficiencies in the Monte Carlo simulation of photon and hadronic interactions in the calorimeter. The modeling of the calorimeter response to photons is studied using well-measured physical processes such as Bhabha scattering. We determine the overall uncertainty by varying the energy, angle, and multiplicity requirements imposed on photons. We also check the $\pi^0$-finding efficiency by performing a semi-inclusive analysis of $B_{h2\pi^0}/B_{h\pi^0}$ ($B_{h3\pi^0}/B_{h\pi^0}$) in which we compare the Monte Carlo and data energy spectra of unused photons in events in which one (two) $\pi^0$'s have been reconstructed. We estimate $\pi^0$ reconstruction uncertainties of 4.1%, 8.1%, and 30% for the 2-, 3-, and 4-$\pi^0$ results.

The error due to the $\pi^0$ signal extraction method is estimated by comparing results from $n$-dimensional sideband subtractions and the $\chi^2$ method, and also by considering all $\pi^0$ combinations instead of only the "best" one. Uncertainties in modeling the trigger efficiency are inferred from the data, comparing parallel trigger streams with different energy and tracking requirements. Systematic errors in the hadronic background subtraction are obtained from studies of (hadron-dominated) 3-3 topology events selected with the same criteria as the 1-3 events. The $\tau$ background subtraction is studied by varying the input branching ratios used in the $\tau$ Monte Carlo simulation over a range permitted by existing data [1]. For $B_{h3\pi^0}/B_{h\pi^0}$, significant contributions to the systematic error arise from signal extraction (5.5%) and $\tau$ background (5.0%).

The results from the different tags are averaged, weighted by statistical and independent systematic errors added in quadrature. Errors due to signal extraction, $\pi^0$ reconstruction, and $f_\tau$ are common errors, and we add them in quadrature with the independent systematic errors. We obtain $B_{h2\pi^0}/B_{h\pi^0}=0.345 \pm 0.006 \pm 0.016$, $B_{h3\pi^0}/B_{h\pi^0}=0.041 \pm 0.003 \pm 0.005$, and $B_{h4\pi^0}/B_{h\pi^0}=0.006 \pm 0.002 \pm 0.002$, where the first error is statistical and the second systematic.

Using the world-average value [1] of $B_{h\pi^0}=(23.8 \pm 0.8)$%, we infer absolute branching fractions:

$$B_{h2\pi^0}=(8.21 \pm 0.15 \pm 0.38 \pm 0.28)\% ,$$

$$B_{h3\pi^0}=(0.98 \pm 0.07 \pm 0.12 \pm 0.03)\% ,$$

and

$$B_{h4\pi^0}=(0.15 \pm 0.04 \pm 0.05 \pm 0.01)\% ,$$

where the last uncertainty reflects that of $B_{h\pi^0}$. These results are consistent with (and more precise than) present world averages. They are all lower than the world aver-

TABLE II. Relative probabilities of detecting the modes under study. Errors are statistical only. Decay modes with small branching ratios are not shown.

| Input decay mode | Relative efficiency (%) for detection as $h^\pm \pi^0 \nu$ | $h^\pm 2\pi^0 \nu$ | $h^\pm 3\pi^0 \nu$ | $h^\pm 4\pi^0 \nu$ |
|---|---|---|---|---|
| $h^\pm \nu$ | $0.1 \pm 0.1$ | $<0.1$ | $<0.3$ | $<0.4$ |
| $h^\pm \pi^0 \nu$ | 100 | $0.4 \pm 0.2$ | $<0.3$ | $<0.4$ |
| $h^\pm 2\pi^0 \nu$ | $11.4 \pm 0.4$ | 100 | $0.5 \pm 0.3$ | $<0.4$ |
| $h^\pm 3\pi^0 \nu$ | $1.2 \pm 0.3$ | $17.8 \pm 1.2$ | 100 | $1.1 \pm 0.7$ |
| $h^\pm 4\pi^0 \nu$ | $<0.2$ | $4.0 \pm 0.7$ | $28.0 \pm 4.0$ | 100 |

ages, however, supporting the existence of the "one-prong problem" [12]. In particular, the $\tau \to h^{\pm}2\pi^0\nu_\tau$ result is markedly lower than that from several recent experiments [13,14]. The branching fractions for the $h^{\pm}3\pi^0\nu$ and $h^{\pm}4\pi^0\nu$ modes are consistent with theoretical expectations from CVC (conserved-vector-current hypothesis) and isospin [3,15].

We gratefully acknowledge the effort of the CESR staff in providing us with excellent luminosity and running conditions. J.P.A. and P.S.D. thank the PYI program of the NSF, K.H. thanks the Alexander von Humboldt Stiftung, G.E. thanks the Heisenberg Foundation, K.K.G. and A.J.W. thank the SSC Fellowship program of TNRLC, K.K.G. thanks the OJI program of DOE, and R.P. and P.R. thank the A.P. Sloan Foundation for support. This work was supported by the National Science Foundation and the U.S. Department of Energy.

(a)Permanent address: Carleton University, Ottawa, Canada.

(b)Permanent address: Institute of Nuclear Physics, Novosibirsk, Russia.

[1] Particle Data Group, Phys. Rev. D **45**, 1 (1992).

[2] T. N. Truong, Phys. Rev. D **30**, 1509 (1984).

[3] F. J. Gilman and S. H. Rhie, Phys. Rev. D **31**, 1066 (1985).

[4] Y. Kubota *et al.*, Nucl. Instrum. Methods Phys. Res., Sect. A **320**, 66 (1992).

[5] More restrictive cuts on $\chi^2_{n\pi^0}$ are employed for the three-prong tags to reduce hadronic background.

[6] In the 1-$\pi^0$ case, we evaluate this background assuming it to be linear in $(m_{\gamma\gamma}\text{-}m_{\pi^0})/\sigma_m$; in the 2-, 3-, and 4-$\pi^0$ cases, we take it to be flat in $\chi^2_{n\pi^0}$. We account for possible deviations from these shapes in the systematic error.

[7] S. Jadach and Z. Was, Comput. Phys. Commun. **64**, 267 (1991), and references therein.

[8] Computer code GEANT 3.14, in R. Brun *et al.*, CERN Report No. CERN DD/EE/84-1 (unpublished).

[9] The absolute detection efficiency for $h^{\pm}\pi^0$ events depends on the tag, ranging from 14% to 19%.

[10] Additional components of $f_\tau$ include the $\pi^{\pm}\omega\nu_\tau$ channel and final states with neutral kaons, specifically $\pi^{\pm}K^0$ [from $\tau \to K^{*\pm}(892)\nu_\tau$] and $h^{\pm}K^0\pi^0$. Decays with $K_S \to \pi^0\pi^0$ or $K_L$ which can enter final event samples are thus considered as tau background.

[11] To calculate $f_\tau$ we use the "fit" $\tau$ branching ratios of Ref. [1], and take $B(\tau \to h^{\pm}K^0\pi^0\nu_\tau) = (0.48 \pm 0.48)\%$, based on related decays summarized therein. For the $h^{\pm}4\pi^0\nu$ final state we only consider "feedup" from modes with lower $\pi^0$ multiplicity, so our result may include contributions from final states such as $h^{\pm}5\pi^0\nu$.

[12] Using our exclusive branching fractions for the multi-$\pi^0$ modes and the world averages for all other one-prong modes yields a one-prong deficit of $(4.4 \pm 1.3)\%$.

[13] ALEPH Collaboration, D. Decamp *et al.*, Z. Phys. C **54**, 211 (1992).

[14] CELLO Collaboration, H. J. Behrend *et al.*, Z. Phys. C **46**, 537 (1990).

[15] The $h^{\pm}4\pi^0\nu$ result includes a contribution from the decay $\tau^{\pm} \to \pi^{\pm}\eta\pi^0\nu_\tau$, with $\eta \to \pi^0\pi^0\pi^0$, expected at $(0.06 \pm 0.01)\%$, based on the direct study of this $\tau$ decay using $\eta \to \gamma\gamma$, $\pi^+\pi^-\pi^0$, and $\pi^0\pi^0\pi^0$; see CLEO Collaboration, M. Artuso *et al.*, Phys. Rev. Lett. **69**, 3278 (1992).